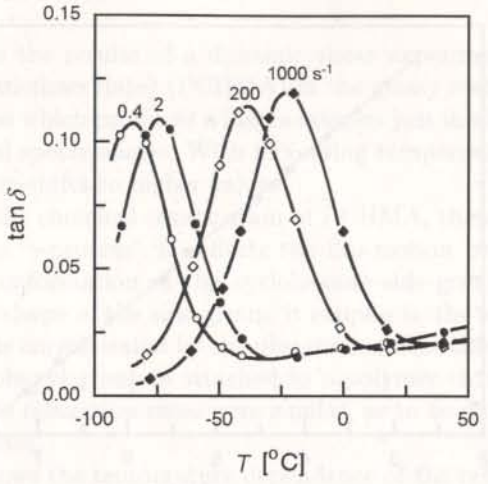


**Fig. 5.9.** Temperature dependent measurements of the loss tangent of the $\gamma$-process of PCHMA for several fixed frequencies $\omega/2\pi$ (After Heijboer [49])

What is applied here is known in the literature as the 'time-temperature superposition principle'. The result of the synthesis is called a 'master-curve'. For a thermally activated Debye-process, the basis of the principle is easily seen. According to Eq. (5.65), the dynamic compliance and the dynamic modulus here are functions of the product $\omega\tau$, or equivalently, of $\log\omega\tau$ . If we also use Eq. (5.93), we may then represent the compliance as a function of a sum of terms

$$J^*(\log\omega\tau) = J^*\left(\log\omega + \log\tau_0 + \frac{\tilde{A}}{\tilde{R}T}\log e\right) \qquad (5.94)$$

The expression tells us that there are two ways of achieving a change in $J^*$, namely either by a shift in $\log\omega$, or by a shift in $T^{-1}$. The effects of frequency and temperature thus appear as 'superposed', and Eq. (5.94) informs us about the correspondencies.

As a prerequisite for the construction of a master-curve, the shape of the loss curve must remain constant under temperature variations. For the system under discussion, this is obviously fulfilled. Measured curves coincide after appropriate shifts along the $\log\omega$-axis, as is shown in Fig. 5.10 for the real and imaginary part of the dynamic shear modulus. The example represents an ideal case, and here there is also no need for a synthesis of the curves from parts. In many other cases, however, construction of the master-curve is the only means to explore a group of relaxation processes in total. Even if one is not sure if curve shapes are really temperature independent, construction of a master-curve remains useful as it can always provide a rough overall view, good for qualitative purposes.



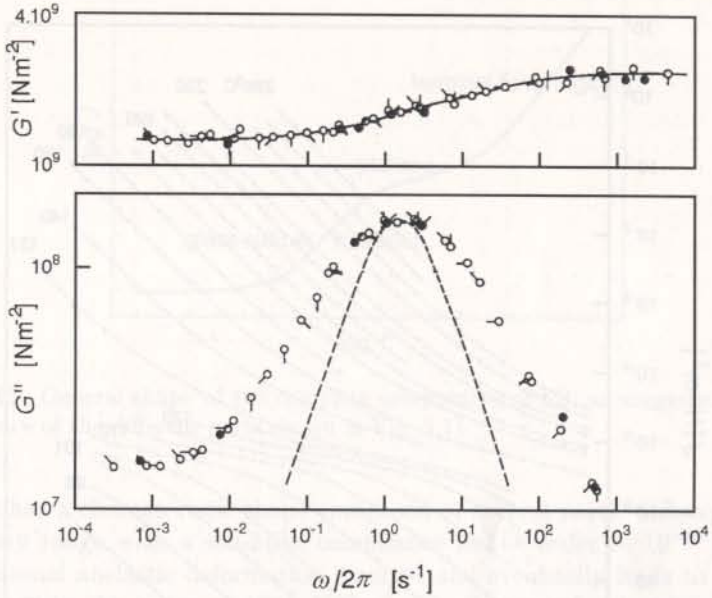


**Fig. 5.10.** Real and imaginary part of the dynamic shear modulus in the range of the $\gamma$-process of PCHMA, synthesized as a master-curve using measurements at various temperatures. Curves represent the viscoelastic behavior at $-80\,^\circ$C. The dashed curve indicates a perfect Debye-process. Data from Heijboer [50]

Figure 5.10 shows also a comparison with the Debye-process. We notice that the $\gamma$-process of the cyclohexyl groups does not agree with a single-time relaxation process, but exhibits some broadening. This may be caused by a coupling between adjacent side-groups, as a conformational change in one side-group may well affect the neighbors. More specifically, the jump rate could depend on the conformations of the neighbors, which then would lead to a distribution of relaxation times, as is indicated by the broadened loss spectrum.

### 5.3.2 Glass-Rubber Transition and Melt Flow

Figure 5.11 presents creep curves, registered for a sample of polystyrene under shear-stress at various temperatures between $-268\,^\circ$C and $296.5\,^\circ$C. We observe a creep compliance which encompasses the enormously broad range of nine orders of magnitude. At the lowest temperatures, the mechanical properties are those of a glass. At the other limit, the high temperature end, the behavior is dominated by viscous flow as indicated by the characteristic linear increase of $J$ with time. The transition from the solid-like to the liquid-like behavior occurs continuously, and most importantly, obviously in a system-

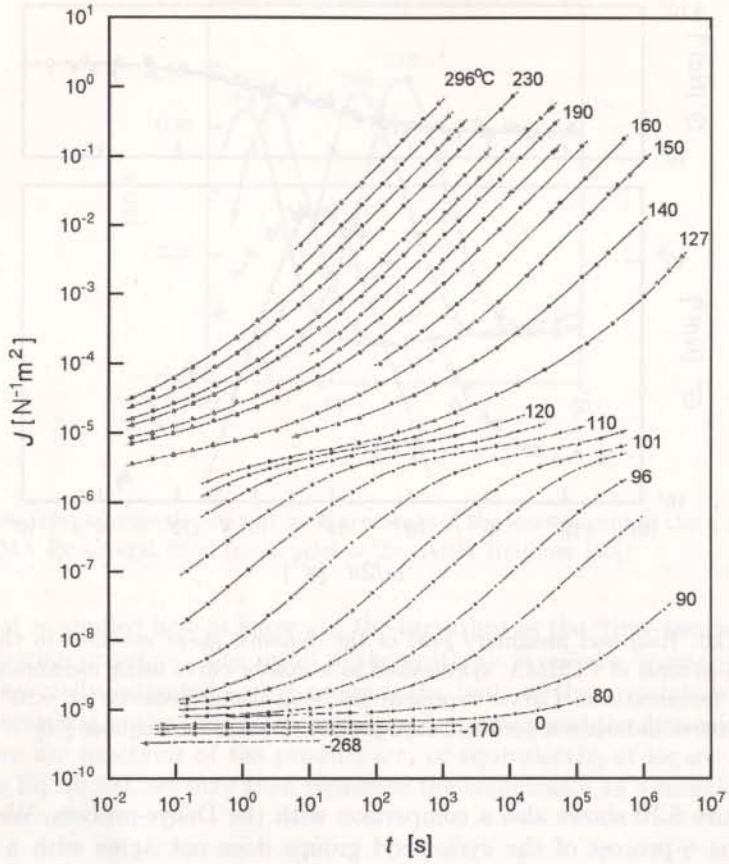


**Fig. 5.11.** Creep compliance of PS ($\overline{M}_w = 3.85 \cdot 10^5$), as measured at the indicated temperatures. Data from Schwarzl [51]

atic manner. Indeed, the way curves change with temperature indicates that again time-temperature superposition is obeyed. Temperature variations result in shifts of the creep compliance along the $\log t$-axis, apparently without essential modifications in shape. The consequence is the same as for the just discussed local processes: On varying the temperature, different parts of $J(t)$ show up in the time-window of the experiment, and they can be reassembled to form a master-curve. Applying this procedure yields the overall creep curve and it evidently has a shape as is indicated schematically in Fig. 5.12. We can estimate the encompassed total time range by roughly summing up the time ranges of the sections included and we find an enormous extension of about 20 orders of magnitude.



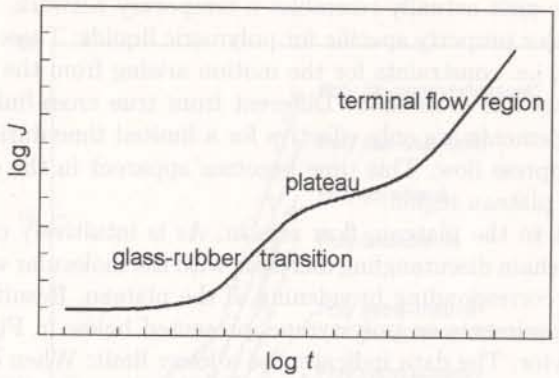


**Fig. 5.12.** General shape of the complete creep curve of PS, as suggested by the appearance of the different parts shown in Fig. 5.11

$J(t)$ has a characteristic shape composed of several parts. Subsequent to the glassy range with a solid-like compliance in the order of $10^{-9}$ $N^{-1}m^2$, an additional anelastic deformation emerges and eventually leads to a shear compliance in the order of $10^{-5}$ $N^{-1}m^2$. The latter value is typical for a rubber. For a certain time a plateau is maintained but then there finally follows a steady linear increase of $J$, as is indicative for viscous flow. The displayed creep curve of polystyrene is really not a peculiar one and may be regarded as representative for all amorphous, i.e. noncrystalline polymers. One always finds these four parts

- a glassy region
- the glass-rubber transition, often also called the '$\alpha$-process'
- a rubber-elastic plateau
- the terminal flow range.

These are the basic ingredients determining the mechanical properties of amorphous polymers and we discuss them now in a brief overview.

A most important conclusion can be drawn immediately and it concerns the nature of the main part, the glass-rubber transition. As we find a systematic shift of the time range of the transition with temperature, it is obvious that we are dealing here with a purely kinetical phenomenon rather than with a structural transition like the melting process or a solid-solid phase change. Curves demonstrate that whether a sample reacts like a glass or a rubber is just a question of time. Temperature enters only indirectly, in that it determines the characteristic time which separates glassy from rubbery behavior.

In chapter 7, we will discuss the properties of rubbers. These are networks, composed of chemically cross-linked macromolecules. Owing to the weak restoring forces, application of stress here induces a deformation which is very large compared to solids. The observation of a plateau in the creep compliance at a height comparable to the compliance of rubbers indicates

that a polymer melt actually resembles a temporary network. This behavior expresses a major property specific for polymeric liquids: These include chain entanglements, i.e. constraints for the motion arising from the chain connectivity, which act like cross-links. Different from true cross-links of chemical nature, entanglements are only effective for a limited time during which they are able to suppress flow. This time becomes apparent in the creep-curve as the end of the plateau region.

Subsequent to the plateau, flow sets in. As is intuitively clear, the time needed for the chain disentangling increases with the molecular weight and this shows up in a corresponding broadening of the plateau. Results of dynamic-mechanical experiments on polystyrene, presented below in Fig. 5.15, exemplify the behavior. The data indicate also a lower limit: When decreasing the molecular weight one reaches a point, where the plateau vanishes. Then the glass-rubber transition and the terminal flow region merge together. Absence of the plateau means the absence of an entanglement network. The observation tells us that entanglement effects only exist above a certain minimum molecular weight. For each polymer one finds a characteristic value, known as the 'critical molecular weight at the entanglement limit', usually denoted $M_c$.

The measurements at high temperatures in Fig. 5.11 indicate a viscous flow with a constant creep rate, determined by a viscosity $\eta_0$

$$\frac{\mathrm{d}J}{\mathrm{d}t} \sim \frac{1}{\eta_0} \tag{5.95}$$

As the flow velocity relates to the disentangling time, this also holds for the melt viscosity. Indeed, $\eta_0$ and the disentangling time for entangled melts show the same dependence on the molecular weight. Figure 5.13 collects the results of viscosity measurements for various polymers. As should be noted, a power law behavior

$$\eta_0 \sim M^{\nu} \tag{5.96}$$

is generally observed. One finds two regions, with different values of the exponent $\nu$ and a cross-over at the entanglement limit $M_c$. For molecular weights below $M_c$ one has $\nu = 1$, above $M_c$ one observes $\nu \approx 3.2 - 3.6$.

Importantly, as is also shown by Fig. 5.15, the two parts of the mechanical response separated by the rubber-elastic plateau differ in their molecular weight dependence. In contrast to the terminal flow region, the glass-rubber transition remains largely unaffected by the molecular weight. The findings teach us that chain equilibration in reaction to an applied field takes place as a two-step process with a finite delay time in between. In the first step equilibration by relaxatory modes only includes chain sequences up to a certain length which is determined by the distance between the entanglements. As this distance is independent of $M$, this holds likewise for the characteristic time of this first step. Further relaxation is postponed until a chain extricates itself from the 'tube' formed by the other surrounding molecules and this process is of course strongly affected by the molecular weight.



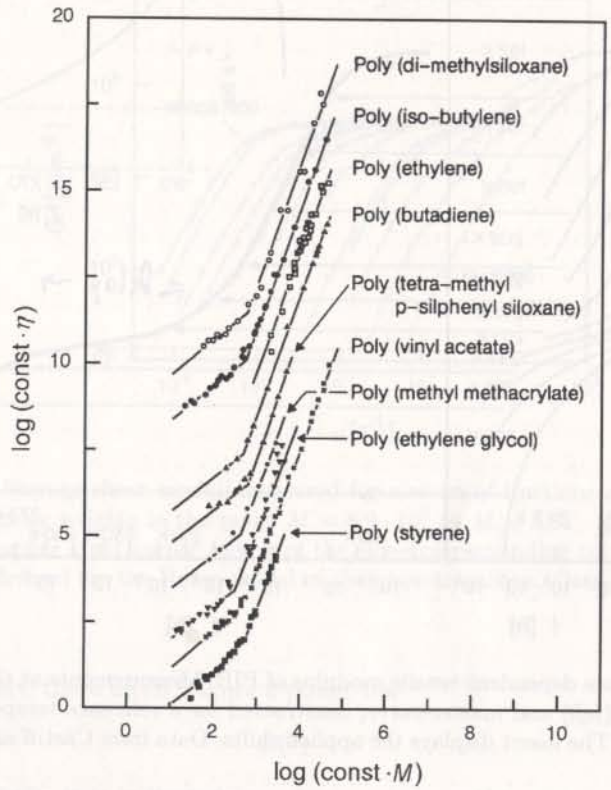


**Fig. 5.13.** Molecular weight dependence of the viscosity as observed for the indicated polymers. For better comparison curves are suitably shifted in horizontal and vertical direction. Data from Berry and Fox [52]

As explained in the first part of this chapter, the viscoelastic properties of polymers may also be studied by stress relaxation experiments or dynamic mechanical measurements. Since all response functions are interrelated, the mentioned ingredients of the mechanical behavior of amorphous polymers must show up in the other experiments as well. To give an example, Fig. 5.14 displays the time dependent tensile modulus registered for polyisobutylene (PIB). Measurements were again conducted for a series of temperatures. As expected, data show the glass-rubber transition (for temperatures in the range 190 – 220 K), followed by a plateau (around 230 K) and finally the onset of flow. The right-hand side presents the composite master-curve, set up by shifting the partial curves as indicated by the arrows. The amounts of shift along the log $t$-axis are displayed in the insert. In the construction of the master-curve the time dependent modulus obtained at 298 K was kept fixed, while all other curves were displaced. The shift factor, denoted log $a_T$,

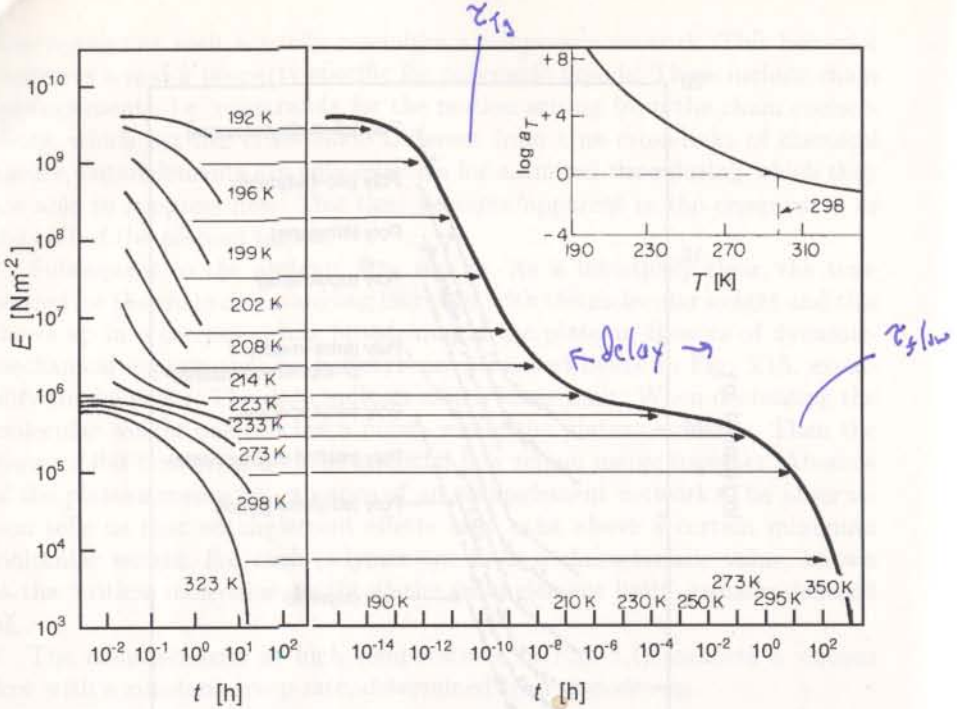


**Fig. 5.14.** Time dependent tensile modulus of PIB. Measurements at the indicated temperatures (*left*) and master-curve, constructed for a reference temperature $T = 298$ K (*right*). The insert displays the applied shifts. Data from Castiff and Tobolsky [53]

is zero at this reference temperature. The result represents the complete time dependent shear modulus at the reference temperature. Comparable to the creep compliance in Fig. 5.12, this tensile modulus again encompasses a huge range of about 20 orders of magnitude in time.

Regarding the large number of conformational changes which must take place if a rubber is to be extended, the glass-rubber transition cannot equal a single-time relaxation process and this is shown by the curve shapes. To describe $E(t)$, empirical equations exist which often provide good data fits. A first one is concerned with the beginning of the transition range. It is known as the 'Kohlrausch-Williams-Watts (KWW)' function and has the form of a 'stretched exponential'

$$E(t) \sim \exp -(\frac{t}{\tau})^{\beta} \tag{5.97}$$

The KWW function employs two parameters: $\tau$ sets the time scale and $\beta$ determines the extension in time of the decay process. For values $\beta < 1$ a broadening results, as is always observed for the glass-rubber transition. Typical values are in the order $\beta \simeq 0.5$. The KWW function holds only at the beginning, i.e. in the short-time range of the glass-rubber transition.



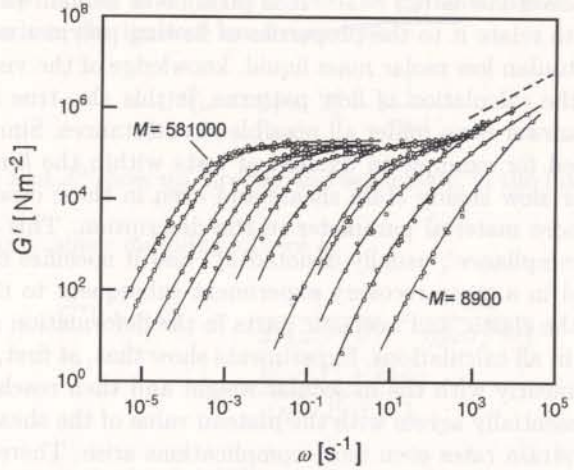


**Fig. 5.15.** Storage shear moduli measured for a series of fractions of PS with different molecular weights in the range $M = 8.9 \cdot 10^3$ to $M = 5.81 \cdot 10^5$. The *dashed line* in the upper right corner indicates the slope corresponding to the power law Eq. (6.81) derived for the Rouse-model of the glass-transition. Data from Onogi et al.[54]

Subsequently, there often follows a power law

$$E(t) \sim t^{-\nu} \tag{5.98}$$

Experimentally it is indicated by a linear range in the center, when using a log-log plot. Typical values of the exponent are $\nu \simeq 0.5$.

Figure 5.15 presents, as a third example, results of dynamic-mechanical measurements. They were obtained for a series of monodisperse polystyrenes, i.e. fractions with sharp molecular weights. The curves depict the frequency dependence of the storage shear modulus, $G'(\omega)$. As we note, the order of appearance of the viscous flow and the $\alpha$-process is reversed when compared to the time dependent measurements. The flow-dominated long-time behavior emerges first at low frequencies, whereas an investigation of the rubber-glass transition requires measurements at the high frequency end. The plateau appears in between. Its width varies systematically with the molecular weight, as already mentioned and discussed. There is no plateau at all for the sample with the lowest molar mass ($M = 8.9 \cdot 10^3$), but after its first appearance, it widens progressively with further increasing molecular weight.

### Low Frequency Properties of Polymer Melts

Also of interest, in Fig. 5.15, is the finding that the shapes of curves in the terminal region remain similar to each other for all molecular weights. More specifically, within the limit of low frequencies, a constant slope emerges,

indicating a power law $G'(\omega) \sim \omega^2$. It is possible to explain this asymptotic behavior and to relate it to the properties of flowing polymer melts.

For a Newtonian low molar mass liquid, knowledge of the viscosity is fully sufficient for the calculation of flow patterns. Is this also true for polymeric liquids? The answer is no under all possible circumstances. Simple situations are encountered for example in dynamical tests within the limit of low frequencies or for slow steady state shears and even in these cases, one has to include one more material parameter in the description. This is the 'recoverable shear compliance', usually denoted $J_e^0$, and it specifies the amount of recoil observed in a creep recovery experiment subsequent to the unloading. $J_e^0$ relates to the elastic and anelastic parts in the deformation and has to be accounted for in all calculations. Experiments show that, at first, for $M < M_c$, $J_e^0$ increases linearly with the molecular weight and then reaches a constant value which essentially agrees with the plateau value of the shear compliance.

At higher strain rates even more complications arise. There the viscosity is no longer constant and shows a decrease with increasing rate, commonly called 'shear-thinning'. We will discuss this effect and related phenomena in chapter 7, when dealing with non-linear behavior. In this section, the focus is on the limiting properties at low shear rates, as expressed by the 'zero shear rate viscosity', $\eta_0$, and the recoverable shear compliance at zero shear rate, $J_e^0$.

Our concern is to find out how the characteristic material parameters $\eta_0$ and $J_e^0$ are included in the various response functions. To begin with, consider a perfectly viscous system in a dynamic-mechanical experiment. Here the dynamic shear compliance is given by

$$J^* = -\mathrm{i}\frac{1}{\eta_0 \omega} \tag{5.99}$$

This is seen when introducing the time dependencies

$$\begin{aligned} \sigma_{zx} &= \sigma_{zx}^0 \exp \mathrm{i}\omega t \\ e_{zx} &= J^* \sigma_{zx}^0 \exp \mathrm{i}\omega t \end{aligned}$$

into the basic equation for Newtonion liquids

$$\sigma_{zx} = \eta_0 \frac{\mathrm{d}e_{zx}}{\mathrm{d}t} \tag{5.100}$$

which results in

$$\sigma_{zx}^0 \exp \mathrm{i}\omega t = \eta_0 \mathrm{i}\omega J^* \sigma_{zx}^0 \exp \mathrm{i}\omega t \tag{5.101}$$

In a polymer melt, the viscous properties of Newtonian liquids combine with elastic forces. The latter ones contribute a real part to the dynamic shear compliance, to be identified with $J_e^0$

$$J'(\omega \to 0) := J_e^0 \tag{5.102}$$



Combining Eqs. (5.99) and (5.102) gives the dynamic shear compliance of polymeric fluids in the limit of low frequencies

$$J^*(\omega \to 0) = J_e^0 - \mathrm{i}\frac{1}{\eta_0 \omega} \tag{5.103}$$

As we see, $\eta_0$ and $J_e^0$ show up directly and separately, in the limiting behavior of $J'$ and $J''$.

The dynamic shear modulus follows as

$$\begin{aligned} G^*(\omega \to 0) &= \frac{1}{J^*(\omega \to 0)} = \frac{\eta_0 \omega}{\eta_0 \omega J_e^0 - \mathrm{i}} \\ &= \frac{\eta_0^2 \omega^2 J_e^0 + \mathrm{i}\eta_0 \omega}{(\eta_0 \omega J_e^0)^2 + 1} \end{aligned} \tag{5.104}$$

giving

$$G'(\omega \to 0) = J_e^0 \eta_0^2 \omega^2 \tag{5.105}$$

in agreement with Fig. 5.15, and

$$G''(\omega \to 0) = \eta_0 \omega \tag{5.106}$$

We thus find characteristic power laws also for the storage and the loss modulus which again include $J_e^0$ and $\eta_0$ in a well-defined way.

One may wonder if $\eta_0$ and $J_e^0$ can also be deduced from the time dependent response functions, as for example from $G(t)$. Indeed, direct relationships exist, expressed by the two equations

$$\eta_0 = \int_0^\infty G(t)\mathrm{d}t \tag{5.107}$$

and

$$J_e^0 \eta_0^2 = \int_0^\infty G(t) t \mathrm{d}t \tag{5.108}$$

The first relation follows immediately from Boltzmann's superposition principle in the form of Eq. (5.38) when applied to the case of a deformation with constant shear rate $\dot{e}_{zx}$. We have

$$(\mathrm{d}x \hat{=}) \mathrm{d}e_{zx} = \dot{e}_{zx} \mathrm{d}t \tag{5.109}$$

and thus

$$(\psi \hat{=})\ \sigma_{zx} = \dot{e}_{zx} \int_{t'=-\infty}^{t} G(t-t')\mathrm{d}t' = \dot{e}_{zx} \int_{t''=0}^{\infty} G(t'')\mathrm{d}t'' \tag{5.110}$$

Since per definition

$$\sigma_{zx} := \eta_0 \dot{e}_{zx}$$

we find

$$\eta_0 = \int_{t=0}^{\infty} G(t)\mathrm{d}t$$

To derive the second equation, we consider a dynamic-mechanical experiment and treat it again on the basis of Boltzmann's superposition principle, writing

$$\sigma_{zx} = \int_{t'=-\infty}^{t} G(t-t')\dot{e}_{zx}(t')\mathrm{d}t' \tag{5.111}$$

Introducing

$$e_{zx}(t) = e^0_{zx} \exp \mathrm{i}\omega t \tag{5.112}$$

and

$$\sigma_{zx}(t) = G^* e_{zx}(t) \tag{5.113}$$

we obtain

$$G^* = \int_{t''=0}^{\infty} G(t'')\mathrm{i}\omega \exp -\mathrm{i}\omega t''\mathrm{d}t'' \tag{5.114}$$

setting $t'' := t - t'$. In the limit $\omega \to 0$ we can use a series expansion

$$G^*(\omega \to 0) = \int_{t''=0}^{\infty} G(t'')(\mathrm{i}\omega + \omega^2 t'' + \ldots)\mathrm{d}t'' \tag{5.115}$$

giving

$$G'(\omega \to 0) = \omega^2 \int_{t=0}^{\infty} G(t)t\mathrm{d}t \tag{5.116}$$

Comparison with Eq. (5.105) yields Eq. (5.108).

Combination of Eqs. (5.107) and (5.108) can be used for estimating the average time of stress decay subsequent to a sudden shear deformation of a melt. We may introduce this time, denoted $\bar{\tau}$, as

$$\bar{\tau} := \frac{\int_{t=0}^{\infty} G(t)t\mathrm{d}t}{\int_{t=0}^{\infty} G(t)\mathrm{d}t} \tag{5.117}$$

and then obtain simply

$$\bar{\tau} = J^0_e \eta_0 \tag{5.118}$$



Equation (5.118) for the mean viscoelastic relaxation time may be applied for both non-entangled and entangled melts and yields different results for the two cases. For non-entangled melts, i.e. $M < M_c$, we have $J^0_e \sim M$ and $\eta_0 \sim M$, hence

$$\bar{\tau} \sim M^2 \tag{5.119}$$

For molecular weights above the entanglement limit, i.e. $M > M_c$, one finds $J^0_e$=const and $\eta_0 \sim M^{3.4}$, therefore

$$\bar{\tau} \sim \eta_0 \sim M^{3.4}. \tag{5.120}$$

### Vogel-Fulcher Law and WLF Equation

We turn now to another important point and consider the temperature dependence. Recall that the data indicate the validity of time-temperature or frequency-temperature superposition. This has an important implication: The findings show that the processes comprising the terminal flow region and the glass-rubber transition change with temperature in the same manner. Particularly suited for the description of this common temperature dependence is the shift parameter $\log a_T$. We introduced it in connection with the construction of the master-curves but it has also a well-defined physical meaning. This becomes revealed when we look at the equations valid in the terminal range, Eqs. (5.105) and (5.106). It should be noted that $\omega$ and $\eta_0$ enter into the expressions for the dynamic modulus and the dynamic compliance not separately, but only as a product. As temperature affects just $\eta_0$, we conclude that $a_T$ and $\eta_0$ must be proportional quantities. The exact relationship follows when taking into account that shift parameters always relate to a certain reference temperature. Let this reference temperature be $T_0$. Then $a_T$ is given by

$$a_T = \frac{\eta_0(T)}{\eta_0(T_0)} \tag{5.121}$$

With the aid of $a_T$ we can express response functions at any temperature in terms of the respective response function at $T_0$. Explicitly, for the dynamical shear modulus, the following relation holds

$$G^*(T,\omega) = G^*(T_0, a_T\omega) \tag{5.122}$$

or for a logarithmic frequency scale

$$G^*(T, \log\omega) = G^*(T_0, \log\omega + \log a_T) \tag{5.123}$$

In correspondence to this, we write for the time dependent shear modulus

$$G(T,t) = G(T_0, \frac{t}{a_T}) \tag{5.124}$$

or

$$G(T, \log t) = G(T_0, \log t - \log a_T) \tag{5.125}$$